ELEMENTA
Science of the Anthropocene

Dawson, HM, et al. 2020. Potential of temperature- and salinity-driven shifts in diatom compatible solute concentrations to impact biogeochemical cycling within sea ice. *Elem Sci Anth,* 8: 25. DOI: https://doi.org/10.1525/elementa.421

RESEARCH ARTICLE

Potential of temperature- and salinity-driven shifts in diatom compatible solute concentrations to impact biogeochemical cycling within sea ice

Hannah M. Dawson*, Katherine R. Heal*, Angela K. Boysen*, Laura T. Carlson*, Anitra E. Ingalls* and Jodi N. Young*

Sea-ice algae are an important source of primary production in polar regions, yet we have limited understanding of their responses to the seasonal cycling of temperature and salinity. Using a targeted liquid chromatography-mass spectrometry-based metabolomics approach, we found that axenic cultures of the Antarctic sea-ice diatom, *Nitzschia lecointei*, displayed large differences in their metabolomes when grown in a matrix of conditions that included temperatures of –1 and 4°C, and salinities of 32 and 41, despite relatively small changes in growth rate. Temperature exerted a greater effect than salinity on cellular metabolite pool sizes, though the N- or S-containing compatible solutes, 2, 3-dihydroxypropane-1-sulfonate (DHPS), glycine betaine (GBT), dimethylsulfoniopropionate (DMSP), and proline responded strongly to both temperature and salinity, suggesting complexity in their control. We saw the largest (> 4-fold) response to salinity for proline. DHPS, a rarely studied but potential compatible solute, had the highest intracellular concentrations among all compatible solutes of ~85 mM. When comparing the culture findings to natural Arctic sea-ice diatom communities, we found extensive overlap in metabolite profiles, highlighting the relevance of culture-based studies to probe environmental questions. Large changes in sea-ice diatom metabolomes and compatible solutes over a seasonal cycle could be significant components of biogeochemical cycling within sea ice.

Keywords: Sea ice; Metabolomics; Diatom; Osmoprotection; Cryoprotection; Metabolism

Introduction

Sea ice is one of the most extensive habitats on Earth, accounting for 15–22 million km^2, or 4.1–6.1%, of global ocean area throughout the year (Arrigo et al., 2014). This unique biome is host to diverse microbial assemblages, including unicellular microalgae that are able to exploit microhabitats produced during sea-ice formation and aging (Arrigo, 2016). Sea-ice algae contribute to carbon fixation via photosynthesis in polar ecosystems, fixing an estimated 10–36 Tg C year^{-1} in the Arctic and 24–36 Tg C year^{-1} in the Antarctic, 2–10% and 1–3% of total annual production (ice + water column) in those regions, respectively (Arrigo, 2016). Though a relatively low fraction of annual production, sea-ice algae are a major source of fixed carbon for higher trophic levels in ice-covered waters, particularly through winter months (Horner and Schrader, 1982; Kottmeier and Sullivan, 1987; Arrigo, 2016; Kohlbach et al., 2017; O'Brien, 1987), and may act as a seeding population for highly productive summertime phytoplankton blooms (Lizotte, 2001; Riaux-Gobin et al., 2011; Tedesco et al., 2012; Arrigo, 2016). Sea-ice algae play an important role in polar biogeochemical cycling of carbon and other nutrients as well as climate-active gas production, namely dimethyl sulfide (DMS) and methane production mediated by bacterial transformations (Welsh, 2000; Vancoppenolle et al., 2013).

Sea-ice algae inhabit the underside of sea ice and its interior, within liquid brine inclusions formed by the exclusion and concentration of salt ions during ice formation (Hsiao, 1980; Horner and Schrader, 1982; Eicken, 1992). Seasonal cycles of ice formation and loss make this habitat both extreme and variable with respect to temperature, salinity, light and nutrients (Dieckmann and Thomas, 2002; Ewert and Deming, 2014). Diatoms dominate sea ice (Horner, 1985; Arrigo, 2014), with pennate diatoms (e.g., *Nitzschia*, *Fragilariopsis*, *Navicula*) being the most common (Günther and Dieckmann, 2001; Fiala et al., 2006).

One strategy diatoms use to mitigate thermal and osmotic stress is accumulating compatible solutes to high intracellular concentrations. Compatible solutes are used by cells of numerous organisms including animals, plants and microorganisms (Welsh, 2000; Chen and Murata, 2002; Yancey, 2005). Most compatible solutes are neutral

* School of Oceanography, University of Washington, Seattle, WA, US

Corresponding author: Hannah M. Dawson (hmdawson@uw.edu)

at physiological pH, either zwitterionic or uncharged (Yancey, 2005), and generally fall into four major classes: free amino acids and derivatives, quaternary ammonium compounds, tertiary sulfonium compounds, and sugars or sugar alcohols (Slama et al., 2015). Compatible solutes can be accumulated to high concentrations without interfering with biochemical processes and can confer osmoprotection by maintaining turgor pressure and stabilizing enzymes (Yancey et al., 1982). Compatible solutes can also aid in cryoprotection by reducing the intracellular freezing point and helping maintain the protein hydration sphere, effectively a layer of free water around the protein, thus stabilizing the tertiary structure of cytosolic enzymes (Welsh, 2000; Lyon and Mock, 2014).

Polar marine diatoms produce a number of compatible solutes, including the sulfur-containing dimethylsulfoniopropionate (DMSP) and isethionic acid (Kirst et al., 1991; Boroujerdi et al., 2012; Lyon et al., 2016) and nitrogen-containing glycine betaine (GBT), proline, and homarine (Krell et al., 2007; Boroujerdi et al., 2012). Many compatible solutes also have other functions (e.g., proline is an amino acid), such that discerning the particular intracellular role(s) they are serving at any time may be difficult. For the purpose of this study on temperature and salinity, we use the term compatible solute broadly to refer to all metabolites that have been reported previously to display osmo- and/or cryoprotective capacity.

The production of high concentrations of compatible solutes, which requires considerable resources and energy, may influence cellular metabolism and resource allocation (Dickson and Kirst, 1987; Welsh, 2000; Spielmeyer and Pohnert, 2012). For example, the polar marine diatom *Fragilariopsis cylindrus* accumulates proline in excess of 15 fmol $cell^{-1}$, approximately 150 mM, when grown at salinity 70 (Krell et al., 2007), and GBT can exceed 100 mM concentrations in mesopelagic phytoplankton (Spielmeyer and Pohnert, 2012). Highly abundant compatible solutes can also be released rapidly from marine algal and bacterial cells into the environment in response to relatively large salinity downshifts (>14) (Fulda et al., 1990; Firth et al., 2016; Torstensson et al., 2019). Once in the surrounding environment, microalgal-produced compatible solutes can be taken up by other members of the microbial community, such as heterotrophic bacteria, for the purpose of osmoregulation (Kiene and Hoffmann Williams, 1998; Spielmeyer et al., 2011) or as a source of carbon, nitrogen or energy (Welsh, 2000; Durham et al., 2019). This catabolism of compatible solutes by bacteria can lead to the production of climate-active gases such as DMS from DMSP (Kirst et al., 1991; Lyon et al., 2011). Additionally, the production and release of sulfur-containing compatible solutes may strongly impact the cryptic cycling of sulfur in sea ice and polar surface oceans through preferential exchange with bacterial partners, as suggested for cosmopolitan pelagic diatoms and bacteria (Durham et al. 2015; Durham et al. 2017; Durham et al. 2019). Thus the release and subsequent transformation of abundant compatible solutes may significantly contribute to the well-documented coupling between primary production and microbial heterotrophy in global oceans (Azam and Malfatti, 2007) and alter the flux of organic matter and the resultant balance between remineralization and storage of key elements (C, N, S, etc.) in polar oceans on a seasonal basis.

This study compares the metabolomes of the sea-ice diatom, *Nitzschia lecointei*, when grown in a matrix of conditions that include temperatures of −1 and 4°C, and salinities of 32 and 41. Most studies of compatible solute use in sea-ice diatoms have focused on more extreme shifts in temperature and salinity and/or single compatible solutes; here we focus on a more modest range of conditions that have comparatively little effect on growth, which allows us to better isolate the impacts of temperature and salinity. Although we are focused on compatible solutes, our metabolomics approach detects other metabolites, some of which are also affected by growth conditions. We compare cultures with diatom-dominated Arctic sea-ice communities so that we can infer how the abundance of small, labile organic molecules impacts sea-ice communities and biogeochemical cycling.

Methods

Culture setup and experimental manipulation

The obligately psychrophilic diatom *Nitzschia lecointei* was isolated from Antarctic bottom sea ice in the Amundsen Sea in 2011 by Torstensson et al. (2013). *N. lecointei* grows at temperatures of −2.3 to 8.3°C and salinities of 17 to 55 (Torstensson et al., 2013, 2019) with the highest growth rate measured at 5.1°C. Axenic stock cultures were established and maintained at −1°C and salinity 32 in 0.2 μm filtered artificial seawater (Enriched Seawater, Artificial Water, ESAW, Harrison et al., 1980) enriched with f/2 nutrients with silica (Guillard, 1975). Cultures were illuminated with cool-white lights on a 20:4 h light:dark cycle at 20–25 μmol photons m^{-2} s^{-1} of photosynthetically active radiation (PAR). Strict aseptic technique was used in order to maintain axenic cultures. Prior to experimental manipulations, cultures were checked for bacterial presence using DAPI fluorescent staining.

For experiments, cultures were grown in acid-washed, combusted borosilicate glass culture tubes. Axenic cultures were inoculated at a density of 7,000 cells mL^{-1}. Desired salinity of media was achieved by dilution or concentration of ESAW salt mix and confirmed by refractometry. Triplicate cultures (each replicate consisting of two pooled samples of 35 mL for 70 mL total per replicate) were grown in a matrix of two temperatures (−1°C and 4°C) and two salinities (32 and 41). Cultures were grown at −1°C in a Percival Scientific LT-36VL Low Temperature Chamber. Cultures were grown at 4°C in a custom-built insulated aquarium tank. Both setups were side-illuminated with cool-white lights at saturating light levels, 20–25 μmol photons m^{-2} s^{-1} and 20:4 h light:dark cycle. Temperatures for both setups were monitored throughout the experiment using Onset HOBO pendant data loggers.

Growth was monitored by relative fluorescence units (RFU) and cultures were sampled for metabolomics during exponential phase on day 21 of growth. Using combusted glassware and gentle vacuum filtration, cells were filtered onto 47 mm 0.2 μm Omnipore Membrane PTFE

filters. Samples were kept on ice during the filtration process. Filters were stored in combusted aluminum foil and immediately frozen at –80°C until extraction. In separate, but identical experiments, RFU was measured in triplicate along with cell diameter and photosynthetic efficiency while carbon and nitrogen content was measured in quadruplicate. The similarity of RFU values and growth phase upon sampling between both sets of experiments supported making direct comparisons between experiments. Based on the tight correlation between RFU and cell number from this identical replicate experiment ($R^2 > 0.9$; Figure S1), we converted RFU values from the original experiment to cell numbers as needed for normalization (i.e., metabolite moles per cell, etc.). RFU was measured at the same time each day, after 15 min of dark incubation and brief gentle mixing, by a Turner Designs TD-700 fluorometer. Cell number and diameter were measured using a Beckman Coulter Z2 Coulter Counter. To prevent cell lysis or changes in cell size, subsamples were diluted in isohaline and isothermal media. Photosynthetic efficiency (F_v/F_m) was measured using PAM fluorometry on replicate glass culture tubes that were kept on ice in the dark for 15 min before measurements were taken in a darkened room. F_v/F_m was determined by measuring the minimum fluorescence (F_0) at a low light level and maximum fluorescence (F_m) after a short saturation pulse of measuring light and calculating the variable fluorescence ($F_v = F_m - F_0$). Particulate organic carbon (POC) and nitrogen (PN) samples were filtered through combusted (450°C, 4 h) 25 mm glass fiber filters (GF/F, pore size 0.7 μm pre-combustion) and frozen. Total organic carbon, nitrogen, and hydrogen of these filters was determined using an Exeter Analytical CE-440 CHN analyzer.

Field sampling

Samples were collected from first-year fast sea ice of the Chukchi Sea near Utqiaġvik (formerly Barrow), AK (at 71°22'22.5"N, 156°30'26.3"W) on 08 May 2017. Snow depth was recorded prior to clearing snow from an area of ice approximately 1 m^2. Ice cores were collected using a Kovacs MARK II ice auger of 9-cm internal diameter. For metabolomics, three dedicated cores were collected and the bottom 5-cm sections were placed into acid-clean 3-L polycarbonate tubs. These sections were then allowed to melt in a cold room at 4°C into prefiltered (0.2 μm) artificial brine solution prepared from Sigma sea salts using the isothermal-isohaline approach of Junge et al. (2004) to avoid osmotic shock and cell lysis. Approximately 500 mL of meltwater was filtered for metabolomics as described for cultures. Filtering was performed in a cold room at 4°C. An additional three cores were taken to measure chlorophyll *a* (Chl *a*), F_v/F_m, POC and PN from the bottom 5 cm after isohaline melts, filtering onto combusted GF/F filters and processing as described for cultures. Chl *a* and phaeopigment analyses was performed using un-acidified and acidified samples to correct for phaeopigments (Welschmeyer, 1994) by extracting filters in 90% v/v acetone/water for 24 h in the dark at –20°C and reading Chl *a* concentrations on a Turner Designs TD-700 (UNESCO, 1994). Temperature and salinity profiles were measured from a separate physical core at 5-cm intervals. Nutrients (phosphate, silicate, nitrate, nitrite, and ammonia) were measured on samples from the bottom 5 cm of the same core after direct melt filtered through 0.2 μm syringe filter into acid-cleaned 60-mL Nalgene bottles and frozen at –20°C. Photosynthetically active radiation (PAR) was measured at the time of sampling through a 45° angled core using a Walz US-SQS spherical quantum sensor and ULM-500 light meter. In addition, the bottom 15 cm of three ice cores collected two days prior from a nearby field site (located 50 m away from the primary site and similar in environmental and biological parameters) were used to measure particulate extracellular polysaccharides (EPS) using the phenol-sulfuric acid method as detailed in Krembs et al. (2011), with conversion from glucose-equivalents (standards based on glucose concentrations) to carbon-equivalents.

Extraction and analysis of metabolites

Metabolite extraction, analysis, and data processing were carried out as described in Boysen et al. (2018). Briefly, polar and nonpolar metabolites were extracted using a modified Bligh-Dyer extraction of 1:1 methanol:water for the aqueous phase and dichloromethane for the organic phase (Bligh and Dyer, 1959; Canelas et al., 2009). Only metabolites extracted in the aqueous phase were analyzed for this study. For normalization, some isotope-labeled internal standards were added before and some after extractions, as in Boysen et al. (2018) and listed in Table S1. Samples were stored at –80°C after extraction and before analysis.

Analysis of metabolite extracts was performed using liquid chromatography-mass spectrometry (LC-MS) exactly as in Boysen et al. (2018). Compounds were separated via liquid chromatography with a Waters Acquity I-Class UPLC, using reversed phase (RP) and hydrophilic interaction liquid chromatography (HILIC). Mass spectrometry parameters for targeted analytes were optimized by infusion of a pure metabolite standard for each. Targeted mass spectrometry data were acquired using a Waters Xevo TQ-S triple quadrupole (TQS) with electrospray ionization (ESI) in selected reaction monitoring mode (SRM) with polarity switching. Untargeted mass spectrometry data was acquired using a Thermo QExactive HF (QE) with ESI to quantify compounds that were overloaded on the TQS.

For all metabolite data, peaks were integrated using Skyline for small molecules (MacLean et al., 2010), and integrated peaks were run through an in-house quality control and normalized via best-matched internal standard (B-MIS) normalization as in Boysen et al. (2018). In the culture experiment, peak areas were normalized to RFU measured on the sample from which metabolites were extracted. Field sample data were normalized to moles of POC on each filter, calculated using the measured moles of carbon per liter of meltwater. For metabolites below detection in some but not all treatments, fold changes were calculated by assigning a value corresponding to the limit of detection (3 × peak area for that compound in the blank +100), which underwent B-MIS and biological normalization as above, as in Lu et al. (2019). These numbers therefore represent a conservative estimate of the fold change.

Relative and absolute metabolite abundances

LC-MS peak areas are influenced by both the amount of a compound injected and its ionization efficiency. Thus, the peak area of two compounds within a sample may differ even if their concentrations are the same. However, normalized peak areas of a given compound can be compared between similar samples, here referred to as relative abundance, as they are a measure of the abundance of a compound relative to the biomass in each sample (i.e., peak area per RFU). DMSP may volatilize during sample processing resulting in some loss of this compound. Good agreement among replicates suggests that losses are similar across samples and therefore our measured relative concentrations can be compared across culture treatments as a minimum value. For the majority of metabolites, relative abundance data were collected on the TQS. For a small subset of overloaded metabolites (arginine, DHPS, DMSP, GBT, glutamic acid, glutamine, and proline), relative abundance data were collected on the QE. We were able to calculate absolute concentrations for select metabolites, including proline (in field and culture samples), for which isotopically-labeled standards were added to samples before or after extraction as a part of the internal standard suite (Table S1). All of these calculations of absolute concentration were performed using data from the TQS except for proline, for which we used data from the QE. In addition, we calculated absolute concentrations of DHPS, GBT, and choline (in field and culture samples) as well as homarine, trigonelline, proline betaine, and hydroxyectoine (in field samples only) by standard additions in matrix using the TQS. We express absolute concentrations in culture in terms of femtomole per cell, using the relationship between RFU and cell numbers ($R^2 > 0.9$, Figure S1), as millimolar intracellular concentration, using cell volume calculated from measured cell diameter (Figure S2) and as a concentration per mole of particulate organic carbon (μmol mol C^{-1}) for field and culture comparisons.

Statistical analysis

Measures of general cell physiology (growth rate, photosynthetic efficiency, carbon content, C:N) and the abundance of individual metabolites were analyzed with two-factor analysis of variance (ANOVA) using R Statistical Software. Post-hoc Tukey's HSD (honestly significant difference) tests were used to explore significant relationships between all treatments when a significant interaction effect between temperature and salinity was observed. If no significant interaction was observed, comparisons were made between total averages of each temperature or salinity treatment (i.e., $n = 6$). Detailed statistics from ANOVA are listed in supplemental tables, as indicated throughout. For comparisons of metabolite abundances across the entire targeted metabolome of *N. lecointei*, fold changes and *p* values were calculated using unpaired *t*-tests. For these univariate statistics on the targeted metabolome, *p* values were corrected for false discovery rate (Benjamini and Hochberg, 1995). A probability level of ≤ 0.05 was used in determining statistical significance

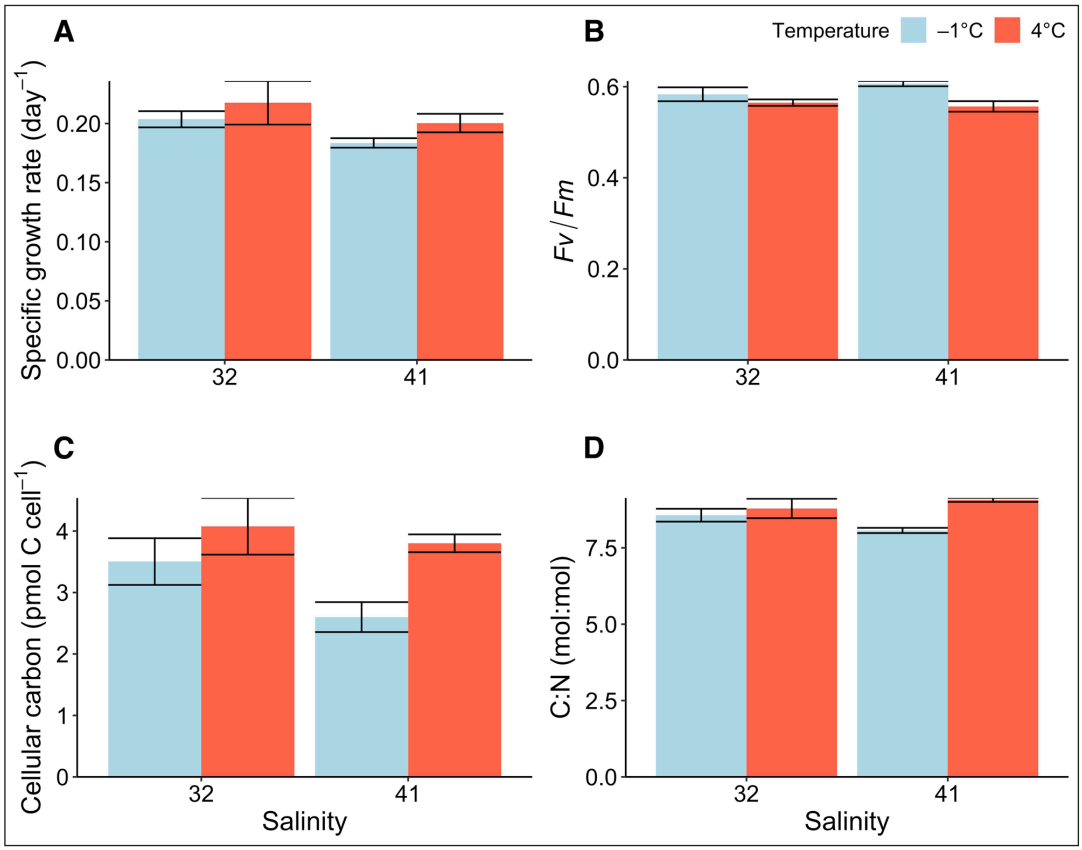

Figure 1: General cell physiology of *Nitzschia lecointei* cultures. a) Specific growth rate (day^{-1}, $n = 3$), **b)** maximum quantum yield (F_v/F_m, $n = 3$, except for 4°C and 32 salinity, where $n = 2$), **c)** carbon per cell (pmol $cell^{-1}$, $n = 4$), and **d)** molar ratio of C:N ($n = 4$). Error bars represent SD. Statistics from two-way ANOVAs are provided in Table S2. DOI: https://doi.org/10.1525/elementa.421.f1

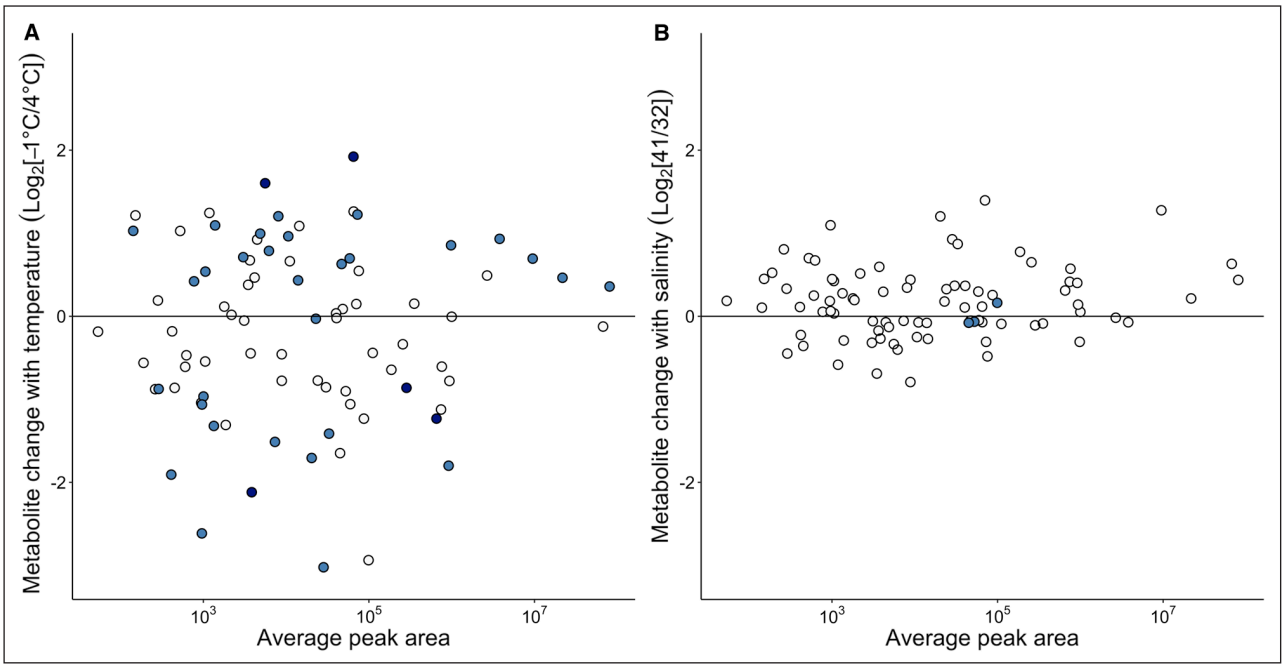

Figure 2: Fold change in relative concentration of metabolites with temperature and salinity. Results of targeted metabolomic analysis of *Nitzschia lecointei*, where treatment effect is expressed as $\log_2$[fold change] in metabolite abundance with **(a)** temperature, at −1°C compared to 4°C, and **(b)** salinity, at 41 compared to 32. Each circle represents a detected metabolite plotted according to its averaged normalized peak area. Compound peak areas were normalized to relative fluorescence units (RFU) before analysis. X-axis is log-scaled. Light blue circles indicate compounds significantly different only under one matching treatment ($p < 0.05$); e.g., in (a), significant differences with temperature at either 32 or 41 salinity. Dark blue circles indicate compounds significantly different under both matching treatments ($p < 0.05$); white circles, no significant differences. DOI: https://doi.org/10.1525/elementa.421.f2

in all analyses. For comparison of absolute concentrations of select metabolites between culture and field samples, a linear regression was used and regression results reported with the adjusted R^2 and *p*-value.

Results

General cell physiology of N. lecointei cultures at different temperatures and salinities

Growth rates and photosynthetic efficiency (F_v/F_m) showed small responses over the range of temperature and salinity tested. Specific growth rates were on average ~10% higher at 4°C compared to −1°C and at lower salinity (32) compared to higher salinity (41) ($p < 0.05$; **Figure 1a**, Table S2). Photosynthetic efficiency (F_v/F_m) was generally high in all treatments, approaching the theoretical optimum for marine microalgae (~0.6, **Figure 1b**; versus 0.65, Schreiber, 2004), though F_v/F_m was 6% higher in cultures grown at −1°C than those grown at 4°C ($p < 0.01$; **Figure 1b**, Table S2). Carbon content per cell was, on average, 30% higher at warmer temperatures compared to colder temperatures, and 20% higher at lower salinity compared to high salinity ($p < 0.001$ and $p < 0.01$, respectively; **Figure 1c**, Table S2). C:N ratios and cell size were also higher at warmer and fresher conditions, concurrent with increased cellular carbon content (**Figure 1d**, Figure S2).

Metabolome changes in N. lecointei at different temperatures and salinities

A total of 84 metabolites (Table S3) were detected in *N. lecointei* with our targeted approach. A full list of targeted analytes searched can be found in Boysen et al. (2018). Of the 84 metabolites detected, 35 were significantly different (unpaired *t*-test, $p < 0.05$) between temperature treatments (**Figure 2a**). Most (30) of these metabolites only responded significantly to temperature under one salinity condition, while five metabolites responded to temperature under both salinity treatments. The direction of change was approximately evenly split, with 20 metabolites increased in the cold (−1°C) and 15 increased in the warm (4°C). In comparison, only three metabolites showed a significant difference between salinity treatments (**Figure 2b**). For these three compounds, relative abundance was significantly higher at salinity 32 when grown at −1°C (**Figure 3**).

The bulk of significant metabolite pool changes were due to changes in temperature at a salinity of 32 (**Figure 3**). Overall, there were more metabolites with a statistically significant change in relative abundance and with a greater magnitude of change with a temperature difference of 5°C than with a salinity change of 9. Of the five metabolites that responded to temperature at both salinities, UDP-glucose and homoserine increased at cold temperatures, whereas methylthioadenosine, aconitic acid, and carnitine decreased.

Many of the metabolites that were enriched under subzero conditions are known to act as compatible solutes for cryo- and osmoprotection (e.g., proline and DMSP) or are precursors of compatible solutes (e.g., methionine, choline, and glutamate), while some well-known compatible solutes, e.g. GBT, did not show significant changes in abundance using our strict definition. Many cofactors (NADP, ADP, NAD, AMP, and FAD) were also

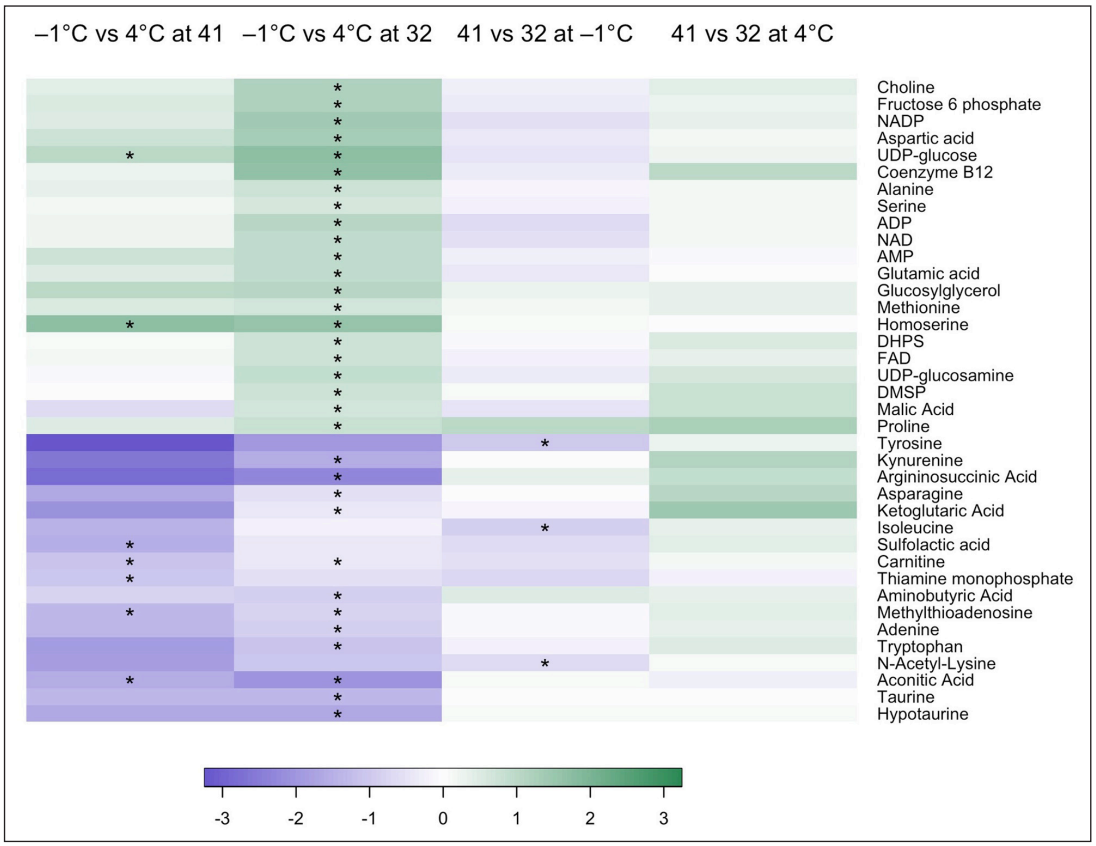

Figure 3: Significant fold changes in relative concentration of metabolites between treatment conditions. Log_2[fold change] of metabolite abundances (normalized metabolite area per relative fluorescence unit) between treatment conditions in *Nitzschia lecointei* cultures for those compounds with one or more significant comparisons (Figure 2), where an asterisk denotes significance ($p < 0.05$). Cell coloration is the log_2[fold change] of average peak size between the different treatments as shown in color key; i.e., average peak size at salinity 41/average peak size at salinity 32 at each temperature, or average peak size at −1°C/average peak size at 4°C at each salinity, as indicated by column name. Thus, green indicates compounds of higher abundance in the −1°C or salinity 41 treatments and purple indicates those of higher abundance in the 4°C or salinity 32 treatments. DOI: https://doi.org/10.1525/elementa.421.f3

enriched. Higher abundances of the coenzyme B_{12} suggests higher uptake from the media since diatoms do not biosynthesize this cofactor. Depleted metabolites at cold temperatures include those involved in the citric acid cycle (e.g., ketoglutaric acid and aconitic acid), along with sulfur-containing metabolites that have been associated with bacterial-algal interactions such as taurine, hypotaurine, and sulfolactic acid (Di Martino et al., 2013; Amin et al., 2015; Landa et al., 2017; Durham et al., 2019; Spietz et al., 2019). Metabolites whose relative abundance differed significantly with salinity did not change significantly with temperature. Isoleucine, N-acetyl-lysine, and tyrosine were all reduced at high salinity at subzero temperature (**Figure 3**).

Comparison of sea-ice diatom metabolomes from cultures and the field

To determine whether a metabolomic analysis of *N. lecointei* cultures could be representative of sea-ice diatom communities, we compared our axenic laboratory culture of *N. lecointei* with a diatom-dominated sea-ice community collected from first-year sea ice near Utqiaġvik, AK, in May 2017 (**Figure 4a**). A dense algal layer was visible within the bottom 5 cm of ice (**Figure 4b**). Light microscopy revealed a diatom-dominated community, with the predominant species being *Nitzschia frigida* (**Figure 4c**), a commonly observed and abundant pennate diatom in both Arctic and Antarctic sea ice (Hsiao, 1980; Horner and Schrader, 1982; Grossi and Sullivan, 1985; Aletsee et al., 1992; Michel et al., 2002), and the same genus as used in our laboratory study. Field data were compared to the *N. lecointei* culture grown at a salinity of 32 and temperature of −1°C, as this treatment experienced conditions closest to the in situ conditions of temperature (−1.3°C), salinity (30). In addition, light intensity (10–50 µmol photons m^{-2} s^{-1}) in the bottom sea ice at the time of collection (morning) closely matched our cultures. F_v/F_m were similar (0.50 ± 0.02 in the field and 0.58 ± 0.02 in cultures) (**Table 1** and **Figure 1b**), as were C:N ratios (9.1 ± 0.1 in the field versus 8.6 ± 0.2 in culture) (**Table 1** and **Figure 1d**).

Within our targeted compounds, more metabolites (104) were detected in the field samples than in the cultures (84) (**Figure 5** inset), though the majority (74) were observed in both sample types. A complete comparison of compounds detected by sample type is provided in Table

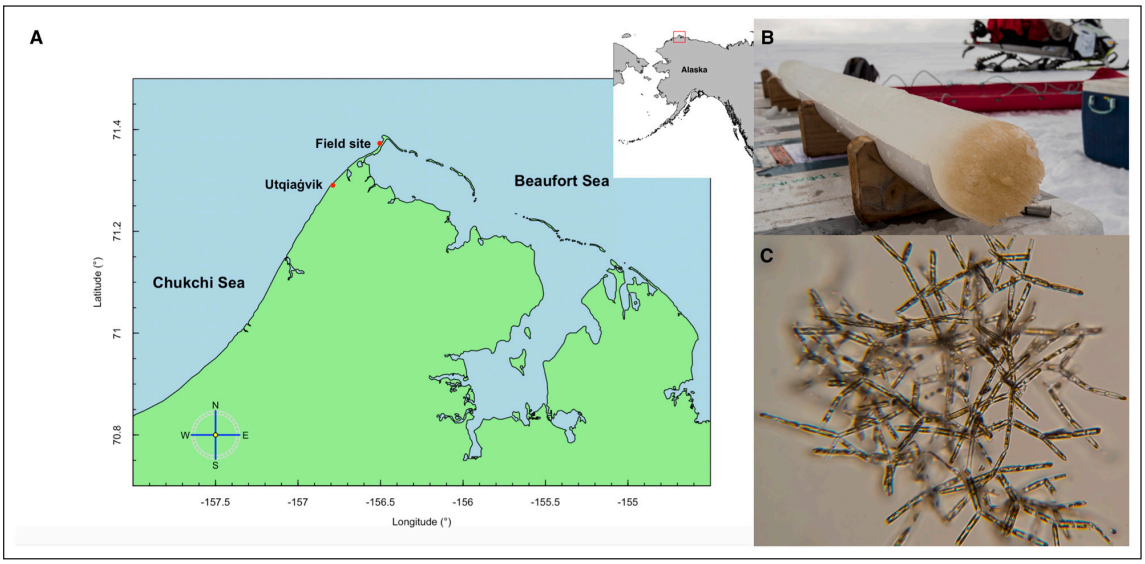

Figure 4: Geographic location and imagery of field site for sea-ice samples collected. (a) Map of field site location near Utqiaġvik with zoom-out inset of Alaska; **(b)** photo by A. Torstensson of sampled ice core with visible bottom algal layer; and **(c)** microscopic image by A. Torstensson of *Nitzschia frigida*, the dominant alga present by visual identification. DOI: https://doi.org/10.1525/elementa.421.f4

S4. While we are unable to compare directly the relative abundances of metabolites between field and culture samples due to different matrix effects in the samples that affect ionization and the challenge of determining biomass in the field where detritus is present, we compare a subset of metabolites for which we obtained absolute concentrations normalized to either cell carbon in culture or moles of POC in the field (**Figure 5** and **Table 2**). We found a strong correlation ($R^2 = 0.87$, $p = 3 \times 10^{-7}$, **Figure 5**), with most metabolites generally 2-fold enriched relative to carbon in the culture than in the field, and compatible solutes DHPS, proline, and GBT were 5- to 8-fold more enriched with respect to carbon in the culture than the field (**Table 2**). Notable exceptions were the metabolites taurine and isethionic acid, which were at higher concentrations in the field than in the culture samples (**Figure 5**). Homarine was at a similar concentration to GBT in the field (see **Table 2**) but was near the detection limit and could not be quantified in the cultures (**Figure 5**). Other potential N- and S-containing compatible solutes that were detected in field samples but were either not detected or quantifiable in culture samples included trigonelline, proline betaine, and hydroxyectoine (**Table 2**), though all at comparatively low concentrations (<15 μmol mol C^{-1}). Variation between triplicate cores was high in the field (**Table 2**), likely due to heterogeneity of algal biomass within sea ice.

A closer look at highly abundant compatible solutes at varying temperature and salinity

Metabolites with the highest measured absolute concentrations in culture and in the field (proline, GBT, and DHPS), and those that fall furthest from the regression line between culture and field samples (homarine, isethionic acid, taurine, methionine) are all N- and/or S-containing compatible solutes or their precursors. It is worth noting that though we did not calculate absolute concentrations of DMSP due to the possibility of evaporation during sample processing, its peak area and estimated ionization efficiency suggest that DMSP could be as or more concentrated than DHPS.

Within our targeted metabolome analysis in **Figure 2**, few metabolites showed significant differences in relative abundance due to salinity. However, this test was highly conservative due to the large number of metabolites analyzed and may have masked more nuanced responses. A closer inspection of the highly abundant compatible solutes (GBT, proline, DHPS and DMSP) using a two-way ANOVA revealed enrichment at both subzero temperatures and higher salinities (**Figure 6**, Table S5) but the pattern and significance of abundance varied between compatible solutes.

Proline, which had intracellular concentrations of 10–50 mM (**Table 3**), responded to both temperature and salinity with no interaction between the two variables. Proline abundance was 142% higher at salinity 41 as compared to salinity 32 ($p < 0.0001$) and 62% higher at −1°C as compared to 4°C ($p < 0.01$; **Figure 6a**, Table S5). Intracellular concentrations of GBT ranged from 30 to 70 mM (**Table 3**) and displayed an interactive response to temperature and salinity (**Figure 6b**). GBT concentration doubled at salinity 41 as compared to 32 when grown at 4°C ($p < 0.001$, Table S5) but not at −1°C. GBT abundance also increased (33%) at warmer temperatures but only at a salinity of 41 ($p < 0.05$; Table S5), not 32. The precursor to GBT, choline, was only significantly more abundant in response to subzero temperature (**Figure 3**) and was detected at a much lower intracellular concentrations (0.5–1 mM; **Table 3**) than GBT.

DHPS was detected in *N. lecointei* at intracellular concentrations ranging from 45 to 85 mM depending on the treatment, making it the most abundant quantified metabolite (**Table 3**). There was a significant interaction between temperature and salinity for DHPS abundance (Table S5). DHPS abundance

Table 1: Environmental parameters of the bottom sea-ice sections from the Utqiaġvik, AK field site at the time of sampling. DOI: https://doi.org/10.1525/elementa.421.t1

Sampling date	8-May-2017
Snow thickness (cm)	7–10
Ice thickness (cm)	125–128
Ice section sampled	Bottom 5 cm (algal band)
Temperature (°C)	−1.3
Salinity	29.9
Light intensity (μmoles photons m^{-2} s^{-2})	10–50
F_v/F_M [a]	0.50 ± 0.02
Chl a (mg m^{-3})[a]	348 ± 34
POC (mM C)[a]	1.7 ± 0.1
C:N (mol:mol)[a]	9.1 ± 0.1
DOC (μM C)[a]	621 ± 386
NO_3^- (μM)[c]	10.19 ± 0.01
pEPS (μM C)[b]	78

[a] Values are mean ± SD, $n = 3$.
[b] Measured from the bottom 15 cm of ice cores and estimated that all came from the bottom 5 cm.
[c] Values are mean ± SD, $n = 2$.

was 55% higher at salinity 41 compared to 32 when grown at 4°C (**Figure 6d**, $p < 0.05$; Table S5). DHPS abundance was also 81% higher when grown at −1°C as compared to 4°C at a salinity of 32 ($p < 0.01$; Table S5).

The relative abundance of DMSP followed the same general pattern of response to temperature and salinity as DHPS (**Figure 6c**). Changes in DMSP across treatments showed comparatively high abundance in all treatments compared to the warmer and less salty treatment. DMSP abundance was 89% higher at salinity 41 as compared to 32 when grown at 4°C ($p < 0.01$; Table S5) but not at −1°C. DMSP abundance was also 81% higher when cells were grown at −1°C as compared to 4°C at a salinity of 32 ($p < 0.01$; Table S5) but not at 41. The intracellular concentration of methionine (a precursor to DMSP) was significantly higher in the subzero treatment (**Figure 3**) and its concentration was 0.1–0.2 mM (data not shown).

Discussion

Experimental conditions tested and general cell physiology

Arrigo and Sullivan (1992) suggested that while temperature and salinity are physically co-varying in sea ice, the physiological responses to each factor is independent, for they found that temperature and salinity had a multiplicative but independent effect on Antarctic sea-ice microalgal growth and photophysiology. Our matrix of temperatures (−1°C vs 4°C) and salinities (32 vs 41) reflect conditions sea-ice diatoms may experience in bottom sea ice flushed with seawater and in the water column upon melt, and intentionally included a treatment not matched to the sea-ice environment (4°C and 41) to allow us to disentangle the individual influences of temperature and salinity on metabolite abundances in *N. lecointei*. Our conditions allowed for similar growth in all treatments such that we could examine the impacts of temperature and salinity, rather than growth rate, on metabolite concentrations.

The range of temperature and salinity in our experimental matrix had little effect on growth rate and photophysiology. While a 10% increase in growth rate with a 5°C increase in temperature was smaller than expected based on Arrhenius equations, a growth response curve by Torstensson et al. (2013) suggests that *N. lecointei* has a broad optimum temperature range that may encompass the temperatures we tested. Alternatively, cells may have increased in size at the warmer temperature rather than increasing growth rate, as we observed significant increases in carbon per cell and cell size (**Figures 1** and S2), which could be due to an actual increase in cell size or an increase in the production of cell-associated EPS. EPS production is sensitive to both temperature and salinity for sea-ice microbes (Krembs et al., 2002; Torstensson et al., 2019). We measured pEPS at high concentrations in the field (78 μM carbon; **Table 1**), and when used to correct C:N ratios in our field samples, the mean values were closer to Redfield (7.9 versus 9.1).

Broad metabolome changes in environmental context

The metabolome of *N. lecointei* differed among treatments despite the relatively small changes in cell growth. In particular, 2- to 3-fold changes in millimolar concentrations of compatible solutes highlight the importance of considering the metabolic response of sea-ice algae to changing environments. Temperature had a much greater effect on the metabolome than salinity, which could be due to the direct, and exponential, effect that temperature has on all biochemical reactions via enzyme kinetics, whereas cells

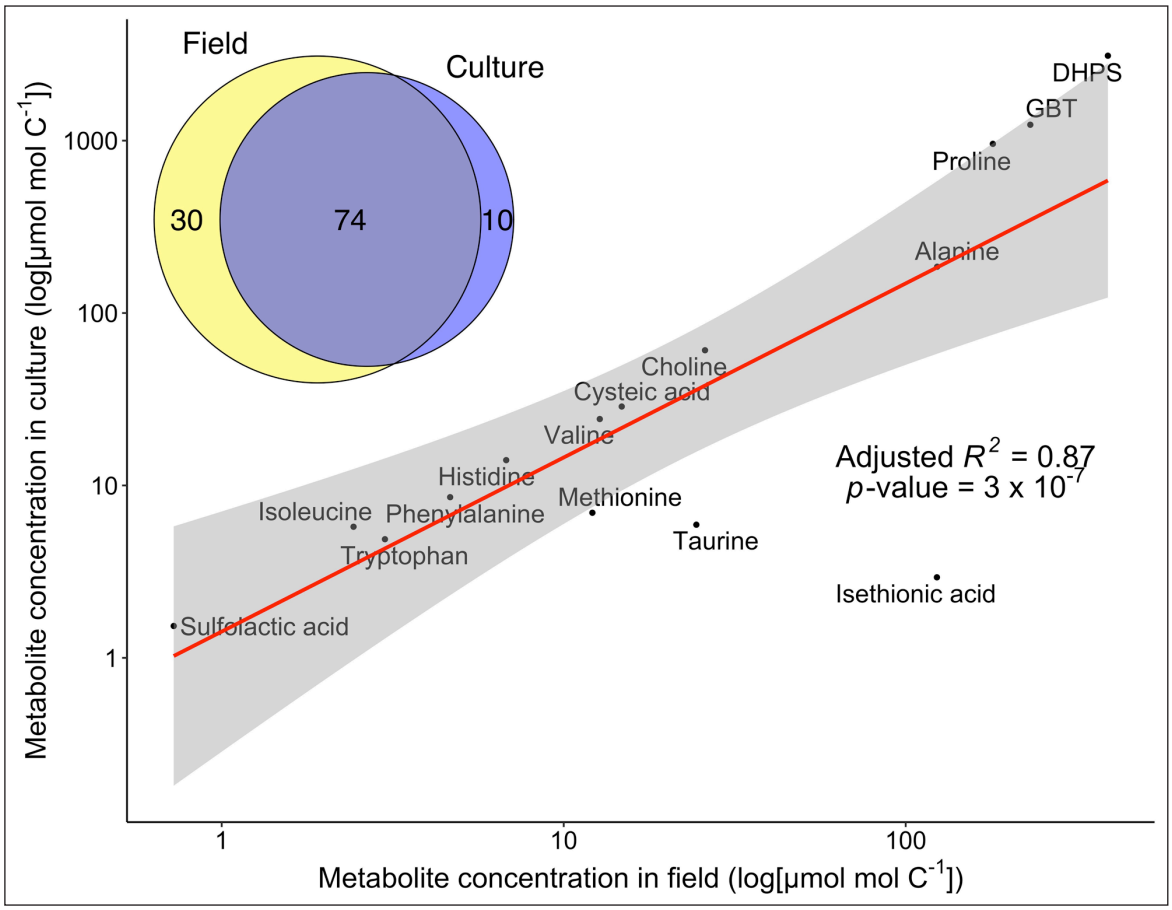

Figure 5: Comparison of culture and field metabolomes. Intracellular concentrations of quantified compatible solutes in *Nitzschia lecointei* cultures grown at salinity 32 and −1°C and field samples of the diatom-dominated mixed community in the bottom 5 cm of sea-ice cores collected from Utqiaġvik, AK. Values are means (n = 3) for all compounds in the culture and field samples. Homarine and trigonelline are not included in this analysis as their concentrations were near the detection limit and not determined in the culture samples, as discussed in the text. Their concentrations in the field samples are available in Table 2. Linear regression statistics are provided on the plot. The shaded area represents a pointwise 95% confidence interval of the fitted values. Axes are log-scaled. Inset is a Venn diagram of targeted metabolites detected in the same *N. lecointei* cultures and field samples. DOI: https://doi.org/10.1525/elementa.421.f5

respond to external changes in salinity by altering key processes to maintain a constant internal osmotic pressure (Yancey et al., 1982). Some compatible solutes can mitigate both temperature and osmotic stress but do so in different ways: cryoprotectants prevent cell freezing via freezing point depression, but do not actively control cell temperature, whereas osmoprotectants actively alter internal osmotic pressure. The stronger response to temperature at 32 salinity compared to 41 may be due to the multiplicative effect of both temperature and salinity; i.e., if metabolites had already responded to high salinity, they might not show as large a response to temperature.

The metabolites with significantly different relative abundances in response to colder temperature, compatible solutes and their precursors, as well as various cofactors, were generally increased. In contrast, those metabolites reduced in abundance were involved in the mobilization of energy reserves (e.g carnitine) and energy production in the citric acid cycle (e.g., ketoglutaric acid and aconitic acid). Also, a number of metabolites implicated in algal-bacterial interaction and nutrient exchange (e.g., tryptophan, taurine, hypotaurine, sulfolactic acid) decreased at the colder temperature. Metabolite pools can change via altered metabolite production or consumption. For metabolites that provide cryoprotection, an increase in pool size would enhance cell survivability, while increases in enzyme cofactors may compensate for slow biochemical reactions at subzero temperatures. Many other organosulfur compounds involved in algal-bacterial interactions may be depleted as resources are redirected to the production of the organosulfur compatible solutes DHPS and DMSP at subzero temperatures. The temperature sensitivity of metabolites that have been associated with algal-bacterial interaction highlights the role temperature may play in dictating these compound-specific interactions in sea-ice environments. Whether the decrease in metabolites involved in energy metabolism is due to slower production or faster depletion of the metabolite pools at cold temperatures is not clear, but, their responses to changing temperature and salinity may help explain how *N. lecointei* is able to maintain its growth rate while challenged with a fluctuating environment.

Table 2: Absolute intracellular concentrations of selected metabolites in the *N. lecointei* culture grown at −1°C and salinity 32 and the Utqiaġvik, AK bottom sea-ice sections. DOI: https://doi.org/10.1525/elementa.421.t2

Compound	Concentration (μmol mol C^{-1})[a]		Fold difference (culture/field)
	Culture	Field	
DHPS	3100 ± 81	390 ± 100	8
GBT	1200 ± 99	230 ± 97	5
Proline	960 ± 80	180 ± 110	5
Alanine	190 ± 17	120 ± 67	2
Choline	61 ± 6.7	26 ± 17	2
Cysteic acid	27 ± 2.2	15 ± 5.0	2
Valine	24 ± 1.4	13 ± 9.5	2
Histidine	14 ± 1.2	6.8 ± 4.0	2
Phenylalanine	8.5 ± 0.15	4.7 ± 2.4	2
Methionine	6.9 ± 0.5	12 ± 8.9	0.6
Taurine	5.9 ± 1.1	24 ± 17	0.2
Isoleucine	5.8 ± 0.43	2.4 ± 0.83	2
Tryptophan	4.9 ± 0.2	3.0 ± 1.4	2
Isethionic acid	2.9 ± 0.35	120 ± 51	0.02
Sulfolactic acid	1.5 ± 0.61	0.72 ± 0.36	2
Homarine	dl[b]	260 ± 110	–
Proline betaine	nd[c]	13 ± 5.7	–
Trigonelline	dl	1.1 ± 0.58	–
Hydroxyectoine	nd	1.1 ± 0.44	–

[a] Values are mean ± SD, $n = 3$. An additional 20% error based on particulate carbon measurement may be present.
[b] At or below detection limit.
[c] Not detected.

Complex response of compatible solutes to environmental change

Compatible solutes with N and S could be significant components of the seasonal cycling of N and S in sea ice. Other compatible solutes, such as many small carbohydrates, are not the focus of this study but could also be important for cryo- and osmoprotection (Greenway and Setter, 1979; Reed et al., 1984; Warr et al., 1984; Ferjani et al., 2003). For example, glucosylglycerol doubled in abundance at the colder culture temperature while sucrose was not significantly affected by either temperature or salinity. We did not quantify these compounds in absolute terms, so cannot comment on their relative contribution to compatible solute pools.

We found GBT, proline, and DHPS in high concentration (μmol mol C^{-1}) in both our culture and field samples. GBT and proline, along with DMSP can act as osmolytes and/or cryoprotectants in polar diatoms (Dieckmann and Thomas, 2002; Krell et al., 2007; Boroujerdi et al., 2012; Lyon and Mock, 2014; Lyon et al., 2016). We detected two other compatible solutes known to occur in diatoms, homoserine (Bromke et al., 2013) and isethionic acid (Boroujerdi et al., 2012), in *N. lecointei*. DMSP, proline, DHPS and GBT had different patterns in response to temperature and salinity which may be due to other metabolic roles beyond osmo- and cryoprotection, constitutive versus inducible regulation, and/or preferential use dependent on cellular resource allocation. The nuanced response of these compounds suggests compatible solutes may play multiple and unique roles in the cell.

In our study, proline showed the largest response, > 4-fold higher at −1°C and salinity 41 compared to 4°C and salinity 32. Even with the 30% salinity increase alone we observed > 2-fold increase in proline. This magnitude of change is comparable to the 4.5-fold increase in proline concentration in *F. cylindrus* in response to a hypersaline shock (a salinity increase of ~100% from 34–70 at 0°C), which was stressful enough to arrest growth temporarily (Krell et al., 2007). Perhaps the large response by *N. lecointei* to seasonal temperature changes may be an important adaptation enabling its success in sea ice. However, while the magnitude of change in proline concentration is similar, intracellular concentrations of proline varied between the two studies — the observed 4-fold increase of proline in *F. cylindrus* estimated as a 30–150 mM increase in intracellular concentration compared to 10–50 mM in *N. lecointei* (**Table 3**). While *N. lecointei* has lower intracellular concentrations of proline, its larger cell

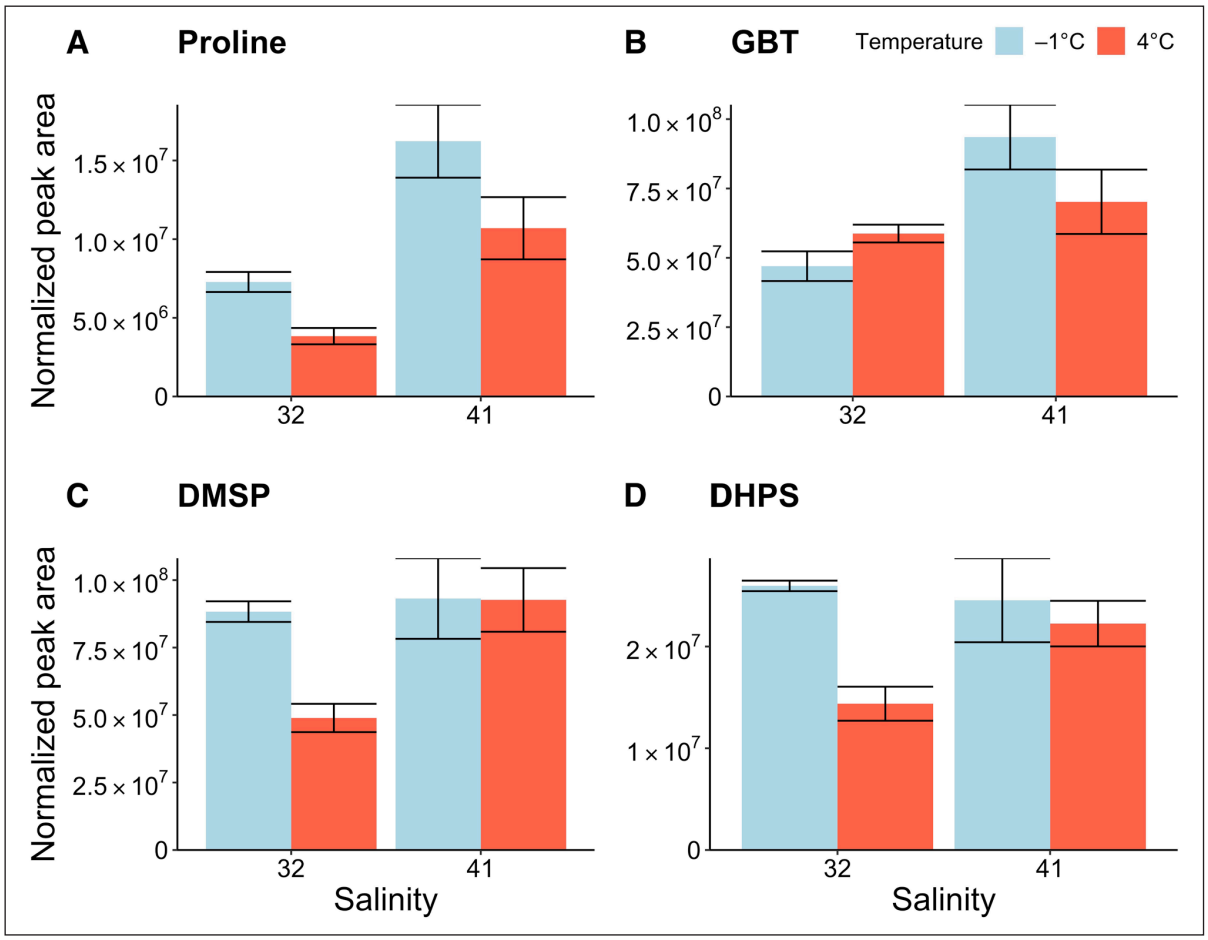

Figure 6: Compatible solute relative concentration changes in response to temperature and salinity. Normalized peak areas (normalized metabolite area per relative fluorescence unit) of compatible solutes in *Nitzschia lecointei* cultures, grouped by each treatment, for **a)** proline, **b)** GBT, **c)** DMSP, and **d)** DHPS. Blue indicates −1°C; orange indicates 4°C. Error bars represent SD ($n = 3$). DOI: https://doi.org/10.1525/elementa.421.f6

size (Olenina et al., 2006; Torstensson et al., 2019) and ability to form dense mats within sea ice means that *N. lecointei* proline production could still be important for biogeochemical cycling.

GBT had intracellular concentrations similar to proline (~30 mM) but was less responsive, doubling in abundance at higher salinity but only at 4°C and no clear response to temperature. GBT may be regulated constitutively or act only as an osmoprotectant in *N. lecointei*. Other evidence implicates GBT as an osmoprotectant in diatoms (Boroujerdi et al., 2012; Torstensson et al., 2019) but as a cryoprotectant only in plants (Chen and Murata, 2002). Torstensson and colleagues found that GBT is taken up from the environment to a greater extent under hypersaline conditions and rapidly expelled from *N. lecointei* during a hypo-osmotic shock (Torstensson et al., 2019), further highlighting the potential import of GBT in biogeochemical cycling.

The two abundant, sulfur-containing compatible solutes, DMSP and DHPS, showed similar patterns of increase with colder temperature and higher salinity, though the response does not appear to be additive. DMSP responds to salinity in other polar microalgae (Lyon et al., 2016) and to temperature in polar macroalgae (Karsten et al., 1996), but little is known about the role of DHPS in polar algae. While we did not quantify the absolute concentration of DMSP in this study, concentrations of 15 mM have been reported in *F. cylindrus* grown at 0°C and a salinity of 35 (Lyon et al., 2016). Surprisingly, the concentrations of DHPS in *N. lecointei* are very high (70–85 mM at salinity 41), approximately 5- to 10-fold greater than has been measured in mesophilic diatom species (Durham et al., 2019) and 2- and 3-fold higher than we measured for GBT and proline, respectively. DHPS was also the most abundant metabolite we quantified in our field samples.

Recent work highlighted the importance of DHPS in sulfur cycling and carbon flux in the surface ocean (Durham et al., 2015, 2017, 2019; Landa et al., 2017, 2019), and its increased abundance with salinity has been noted in the chemoautotrophic bacteria *Sulfurimonas denitrificans* (Götz et al., 2018) and mesophilic diatom *Thalassiosira pseudonana* (Durham et al., 2019). Considering the apparent similarities in the role of DMSP and DHPS as cryo- and osmoprotectants, further investigation is needed to determine whether DHPS production and use could impact the production and release of DMSP, and ultimately the production of the climate-active gas, DMS (Kirst et al., 1991; Welsh, 2000; Lyon et al., 2011; Vancoppenolle et al., 2013). DHPS production may also be connected with the

Table 3: Intracellular concentrations[a] of quantified compatible solutes in cultures of two different sea-ice diatoms at different temperatures and salinities. DOI: https://doi.org/10.1525/elementa.421.t3

Algal taxon	Treatment (S, T)	Proline		DHPS		GBT		Choline	
		(fmol cell^{-1})	(mM)	(fmol cell^{-1})	(mM)	(fmol cell^{-1})	(mM)	(fmol cell^{-1})	(mM)
N. lecointei	31, −1°C[b]	–[c]	–	–	–	6.0 ± 0.4	31.7 ± 2	0.68 ± 0.09	3.6 ± 0.5
N. lecointei	32, −1°C[d]	3.4 ± 0.28	22 ± 1.9	11 ± 0.27	71 ± 1.8	4.3 ± 0.34	28 ± 2.2	0.21 ± 0.023	1.4 ± 0.15
N. lecointei	41, −1°C[d]	7.7 ± 1.2	52 ± 7.3	9.9 ± 1.6	67 ± 11	7.2 ± 0.97	67 ± 11	0.16 ± 0.028	1.1 ± 0.19
N. lecointei	32, 4°C[d]	2.3 ± 0.3	11 ± 1.5	9.1 ± 1.1	45 ± 5.3	6.6 ± 0.55	33 ± 2.8	0.11 ± 0.0087	0.53 ± 0.043
N. lecointei	41, 4°C[d]	5.9 ± 1.1	30 ± 5.8	17 ± 1.7	84 ± 8.5	11 ± 1.6	54 ± 8.2	0.1 ± 0.023	0.53 ± 0.12
F. cylindrus	34, 0°C[e]	3.4	33	–	–	–	–	–	–
F. cylindrus	70, 0°C[e]	15	150	–	–	–	–	–	–
F. cylindrus	70, −4°C[e]	14	130	–	–	–	–	–	–

[a] Values are mean metabolite concentrations ± SD, $n = 3$ unless otherwise noted.
[b] GBT and choline measurements from Torstensson et al. (2019), after 140-h incubation, $n = 2$.
[c] Not reported.
[d] Data from this study, where mM concentrations for *N. lecointei* were based on cell diameter (Figure S2) by Coulter Counter and assumed spherical volume. An additional 5% error based on cell volume estimate may be present.
[e] Proline measurements from Krell et al. (2007), after 20-d incubation, $n = 3$; concentrations calculated using *F. cylindrus* cell volume and carbon content from Olenina et al. (2006).

production and use of isethionic acid, as the biosynthesis routes for both compounds in eukaryotic phytoplankton are linked (Durham et al., 2019). Interestingly, isethionic acid is abundant in *F. cylindrus* (Boroujerdi et al., 2012) and in our field samples, despite its low concentration in *N. lecointei*, suggesting species-specific compatible solute use, even within polar diatoms.

Relevance of sea-ice algal culture work to the sea-ice community

The metabolome in our axenic *N. lecointei* culture showed strong similarities with a sea-ice community dominated by *N. frigida*, with the majority of metabolites found in both sample types and a similar pattern of expression in the subset of metabolites we were able to quantify (for example, DHPS is approximately 3-fold more abundant than proline and GBT, which are of similar concentrations). A notable exception was homarine, and to a lesser extent isethionic acid, which were considerably higher in the field than the *N. lecointei* cultures (near the detection limit). Homarine and isethionic acid may be produced by other diatoms or sea-ice organisms (Nothnagel, 1995; Keller et al., 2004; Boroujerdi et al., 2012; Gebser and Pohnert, 2013; Scholz and Liebezeit, 2012; Fenizia et al., 2020). The lower absolute concentrations of metabolites in the field were likely due to differences in comparing an exponentially growing culture with a mixed sea-ice community that included non-*Nitzschia* diatoms, other organisms, and detrital material collected on a 0.2 μm filter (Horner, 1985; Arrigo et al., 2014; van Leeuwe et al., 2018; Tedesco et al., 2012) that may have diluted the metabolite signals. The overall similarities observed here suggest that results from culture studies can be applied to the field, making targeted metabolomics a powerful approach to tease apart the fine-scale effects of temperature and salinity on the metabolism of sea-ice diatoms.

Potential impact of compatible solutes on N cycling in sea ice

Fluctuations in the intracellular concentration of N-rich compatible solutes in response to environmental shifts could be a significant source/sink of available nitrogen within bottom sea ice. In the case of a sudden salinity downshift, as occurs during ice melt, cold-adapted bacteria have been shown to release compatible solutes rapidly, on subsecond timescales (Firth et al., 2016). Additionally, *N. lecointei* expelled 85% of the intracellular pool of GBT within 68 h following a sudden salinity downshift from 31 to 17 (Torstensson et al., 2019). Assuming proline and homarine have a similar response to salinity downshifts as GBT, an 85% efflux of the intracellular pool of these three compounds, as measured here in the field, during ice melt would equal ~1 μM of compatible solute derived organic nitrogen being released into the equivalent water parcel of a melted 5 cm × 9 cm ice section (see Table S6 for calculation). This concentration of organic nitrogen is about one-tenth of the inorganic nitrate concentration in our field samples (**Table 1**). There are few existing measures of dissolved organic nitrogen (DON) in sea ice, but Retelletti Brogi et al. (2018) measured ~10–15 μM DON in the bottom 15 cm of sea ice in Cambridge Bay (Canadian Arctic) during April–May.

While our estimated organic nitrogen input may be a liberal estimation, it suggests that the release during ice melt of three N-containing compatible solutes alone (less the undefined total pool of nitrogen-containing compatible solutes capable of such efflux) could impact N cycling and heterotrophic production in sea ice considerably, for they could be taken up readily by other organisms and used as compatible solutes (Kiene and Hoffmann Williams, 1998; Spielmeyer et al., 2011; Firth et al., 2016; Torstensson et al., 2019) or as carbon, nitrogen or energy sources (Welsh, 2000; Cherrier and Bauer, 2004). Additionally, respiration of N-containing compatible solutes by sea-ice

bacteria may alter the available ammonium pool in sea ice and fuel nitrification (Firth et al., 2016). The release and recycling of N-containing compatible solutes is likely to be more important to N cycling in oligotrophic regions of the Arctic than the coastal regions, (where our samples were collected), or the Antarctic, where nitrate concentrations in sea ice are generally higher (up to 8 μM in bottom sections and up to 27 μM in gap layers of ice floes (Kattner et al., 2004)). As sea-ice algae are likely producing and releasing these compounds continuously throughout their lives either constitutively or in response to frequent environmental shifts, their cumulative contribution to the dissolved organic matter (DOM) pool may be much larger than the concentration we observe from an instantaneous metabolomic measurement. Characterizing the suite of algal compatible solutes and quantifying their release into the DOM pool is key to fully assessing their importance in biogeochemical cycling in sea ice.

Conclusion

Temperature and salinity change dramatically with the seasonal cycling of sea ice, yet little is known about how sea-ice diatoms are physiologically adapted to survive these changes. Here we have shown that an Antarctic sea-ice diatom, *N. lecointei*, maintains a differentially regulated suite of compatible solutes when grown under temperature and salinity variations well within what they would experience over a seasonal cycle. Many of these compatible solutes were found in similar abundance ratios in a natural bottom sea-ice community, showing the relevance of model organisms in teasing apart complex interactions of factors within sea ice. The varied sensitivity of compatible solute responses suggests that a complex suite of osmo- and cryoprotectant compounds are utilized concurrently to mitigate environmental stress, which in turn may impact biogeochemical cycling and ecosystem dynamics in sea ice over the season. This work highlights that detailed analyses of intracellular composition, such as the metabolomic approach used here, are needed to estimate accurately the impact of cell-level physiological responses of sea-ice algae to temperature and salinity on the surrounding community and environment.

Data Accessibility Statement

Metabolomics data are available in Metabolomics Workbench (https://www.metabolomicsworkbench.org/data/index.php) under Study ID ST001393.

Supplemental file

The supplemental file for this article can be found as follows:

- **Figures S1, S2. Tables S1 – S6.** Supplemental materials for main text. Xlsx. DOI: https://doi.org/10.1525/elementa.421.s1

Acknowledgements

We would like to thank Jody W. Deming for insightful discussion and the opportunity to sample sea ice; Anders Torstensson for providing the axenic culture strain of *N. lecointei*, field photography, and for useful discussions; Bryndan P. Durham for helpful discussions about the role of DHPS; the Ukpeaġvik Iñupiat Corporation Science team for essential logistical support for sea-ice collection; the members of our larger field team for support: Shelly Carpenter, Anders Torstensson, Max Showalter, and Zac Cooper; Regina Lionheart, Alexa Weid, and Natalie Kellogg for assistance with lab work; Viviana Castillo for assistance with lab work; Aaron Morello and the UW Marine Chemistry Lab for assistance with CHN and Chlorophyll analysis; and Megan Schatz and E. Virginia Armbrust for assistance with PAM fluorometry measurements.

Funding information

Funding for this project was provided by the Beatrice Crosby Booth Endowed Fellowship (HMD), University of Washington Graduate Top Scholar Award (HMD), grants from the National Science Foundation (174465, HMD and JNY; OCE-1228770, AEI; GRFP to AKB and KRH) and the Simons Foundation (SF Award ID 385428, AEI; Award ID 598819, KRH), and JNY Start-up funds from the University of Washington, School of Oceanography. The opportunity to sample Arctic sea ice was provided by Jody W. Deming through funding from the Gordon and Betty Moore Foundation, Grant 5488.

Competing interests

We declare no competing interests. We acknowledge interacting with Elementa editor Jody W. Deming for manuscript discussions and opportunities to collect sea-ice samples.

Author contributions

- Contributed to conception and design: HMD, JNY
- Contributed to acquisition of data: HMD, LTC, KRH, AKB
- Contributed to analysis and interpretation of data: HMD, KRH, AKB, AEI, JNY
- Drafted and/or revised the article: HMD, JNY, AEI, KRH, AKB, LTC
- Approved the submitted version for publication: HMD, KRH, AKB, LTC, AEI, JNY

References

Aletsee, L and **Jahnke, J.** 1992. Growth and productivity of the psychrophilic marine diatoms *Thalassiosira antarctica* Comber and *Nitzschia frigida* Grunow in batch cultures at temperatures below the freezing point of sea water. *Polar Biol* **11**(8): 643–647. DOI: https://doi.org/10.1007/BF00237960

Amin, SA, Hmelo, LR, van Tol, HM, Durham, BP, Carlson, LT, Heal, KR, Morales, RL, Berthiaume, CT, Parker, MS, Djunaedi, B, Ingalls, AE, Parsek, MR, Moran, MA and **Armbrust, EV.** 2015. Interaction and signaling between a cosmopolitan phytoplankton and associated bacteria. *Nature* **522**(7554): 98–101. DOI: https://doi.org/10.1038/nature14488

Arrigo, KR. 2014. Sea ice ecosystems. *Ann Rev Mar Sci* **6**(1): 439–467. DOI: https://doi.org/10.1146/annurev-marine-010213-135103

Arrigo, KR. 2016. Sea ice as a habitat for primary producers. In: Thomas, D (ed.), *Sea ice*, 3rd ed., 352–369. Chichester, UK; Hoboken, NJ: John Wiley & Sons. DOI: https://doi.org/10.1002/9781118778371.ch14

Arrigo, KR, Brown, ZW and **Mills, MM.** 2014. Sea ice algal biomass and physiology in the Amundsen Sea, Antarctica. *Elem Sci Anthr* **2**: 000028. DOI: https://doi.org/10.12952/journal.elementa.000028

Arrigo, KR and **Sullivan, CW.** 1992. The influence of salinity and temperature covariation on the photophysiological characteristics of Antarctic sea ice microalgae. *J Phycol* **28**(6): 746–756. DOI: https://doi.org/10.1111/j.0022-3646.1992.00746.x

Azam, F and **Malfatti, F.** 2007. Microbial structuring of marine ecosystems. *Nat Rev Microbiol* **5**(10): 782–791. DOI: https://doi.org/10.1038/nrmicro1747

Benjamini, Y and **Hochberg, Y.** 1995. Controlling the false discovery rate: A practical and powerful approach to multiple testing. *J R Stat Soc* **57**(1): 289 –300. DOI: https://doi.org/10.1111/j.2517-6161.1995.tb02031.x

Bligh, EG and **Dyer, WJ.** 1959. A rapid method of total lipid extraction and purification. *Can J Biochem Physiol* **37**(8): 911–917. DOI: https://doi.org/10.1139/o59-099

Boroujerdi, AFB, Lee, PA, DiTullio, GR, Janech, MG, Vied, SB and **Bearden, DW.** 2012. Identification of isethionic acid and other small molecule metabolites of *Fragilariopsis cylindrus* with nuclear magnetic resonance. *Anal Bioanal Chem* **404**(3): 777–784. DOI: https://doi.org/10.1007/s00216-012-6169-2

Boysen, AK, Heal, KR, Carlson, LT and **Ingalls, AE.** 2018. Best-matched internal standard normalization in liquid chromatography-mass spectrometry metabolomics applied to environmental samples. *Anal Chem* **90**(2): 1363–1369. DOI: https://doi.org/10.1021/acs.analchem.7b04400

Bromke, MA, Giavalisco, P, Willmitzer, L and **Hesse, H.** 2013. Metabolic analysis of adaptation to short-term changes in culture conditions of the marine diatom *Thalassiosira pseudonana*. *PLoS One* **8**(6): e67340. DOI: https://doi.org/10.1371/journal.pone.0067340

Canelas, AB, ten Pierick, A, Ras, C, Seifar, RM, van Dam, JC, van Gulik, WM and **Heijnen, JJ.** 2009. Quantitative evaluation of intracellular metabolite extraction techniques for yeast metabolomics. *Anal Chem* **81**(17): 7379–7389. DOI: https://doi.org/10.1021/ac900999t

Chen, THH and **Murata, N.** 2002. Enhancement of tolerance of abiotic stress by metabolic engineering of betaines and other compatible solutes. *Curr Opin Plant Biol* **5**(3): 250–257. DOI: https://doi.org/10.1016/S1369-5266(02)00255-8

Cherrier, J and **Bauer, JE.** 2004. Bacterial utilization of transient plankton-derived dissolved organic carbon and nitrogen inputs in surface ocean waters. *Aquat Microb Ecol* **35**(3): 229–241. DOI: https://doi.org/10.3354/ame035229

Dickson, DMJ and **Kirst, GO.** 1987. Osmotic adjustment in marine eukaryotic algae: the role of inorganic ions, quaternary ammonium, tertiary sulfonium and carbohydrate solutes. 2. Prasinophytes and Haptophytes. *New Phytol* **106**(4): 657–666. DOI: https://doi.org/10.1111/j.1469-8137.1987.tb00166.x

Di Martino, ML, Campilongo, R, Casalino, M, Micheli, G, Colonna, B and **Prosseda, G.** 2013. Polyamines: Emerging players in bacteria-host interactions. *Int J Med Microbiol* **303**(8): 484–491. DOI: https://doi.org/10.1016/j.ijmm.2013.06.008

Dieckmann, GS and **Thomas, DN.** 2002. Antarctic sea ice–a habitat for extremophiles. *Science* **295**(5555): 641–644. DOI: https://doi.org/10.1126/science.1063391

Durham, BP, Boysen, AK, Carlson, LT, Groussman, RD, Heal, KR, Cain, KR, Morales, RL, Coesel, SN, Morris, RM, Ingalls, AE and **Armbrust, EV.** 2019. Sulfonate-based networks between eukaryotic phytoplankton and heterotrophic bacteria in the surface ocean. *Nat Microbiol* **4**(10): 1706–1715. DOI: https://doi.org/10.1038/s41564-019-0507-5

Durham, BP, Dearth, SP, Sharma, S, Amin, SA, Smith, CB, Campagna, SR, Armbrust, EV and **Moran, MA.** 2017. Recognition cascade and metabolite transfer in a marine bacteria-phytoplankton model system. *Environ Microbiol* **19**(9): 3500–3513. DOI: https://doi.org/10.1111/1462-2920.13834

Durham, BP, Sharma, S, Luo, H, Smith, CB, Amin, SA, Bender, SJ, Dearth, SP, Van Mooy, BAS, Campagna, SR, Kujawinski, EB, Armbrust, EV and **Moran, MA.** 2015. Cryptic carbon and sulfur cycling between surface ocean plankton. *Proc Natl Acad Sci* **112**(2): 453–457. DOI: https://doi.org/10.1073/pnas.1413137112

Eicken, H. 1992. Salinity profiles of Antarctic sea ice: Field data and model results. *J Geophys Res* **97**(92): 15545–15557. DOI: https://doi.org/10.1029/92JC01588

Ewert, M and **Deming, JW.** 2014. Bacterial responses to fluctuations and extremes in temperature and brine salinity at the surface of Arctic winter sea ice. *FEMS Microbiol Ecol* **89**(2): 476–489. DOI: https://doi.org/10.1111/1574-6941.12363

Fenizia, S, Thume, K, Wirgenings, M and **Pohnert, G.** 2020. Ectoine from bacterial and algal origin is a compatible solute in microalgae. *Mar Drugs* **18**(1), 42: 1–13. DOI: https://doi.org/10.3390/md18010042

Ferjani, A, Mustardy, L, Sulpice, R, Marin, K, Suzuki, I, Hagemann, M and **Murata, N.** 2003. Glucosylglycerol, a compatible solute, sustains cell division under salt stress. *Plant Physiol* **131**(4): 1628–1637. DOI: https://doi.org/10.1104/pp.102.017277

Fiala, M, Kuosa, H, Kopczyńska, EE, Oriol, L and **Delille, D.** 2006. Spatial and seasonal heterogeneity of sea ice microbial communities in the first-year ice of Terre Adélie area (Antarctica). *Aquat Microb Ecol* **43**(1): 95–106. DOI: https://doi.org/10.3354/ame043095

Firth, E, Carpenter, SD, Sørensen, HL, Collins, RE and **Deming, JW.** 2016. Bacterial use of choline to tolerate salinity shifts in sea-ice brines. *Elem Sci Anthr* **4**: 000120. DOI: https://doi.org/10.12952/journal.elementa.000120

Fulda, S, Hagemann, M and **Libbert, E.** 1990. Release of glucosylglycerol from the cyanobacterium *Synechocystis* spec. SAG 92.79 by hypoosmotic shock. *Arch Microbiol* **153**(4): 405–408. DOI: https://doi.org/10.1007/BF00249013

Gebser, B and **Pohnert, G.** 2013. Synchronized regulation of different zwitterionic metabolites in the osmoadaption of phytoplankton. *Mar Drugs* **11**(6): 2168–2182. DOI: https://doi.org/10.3390/md11062168

Götz, F, Longnecker, K, Kido Soule, MC, Becker, KW, Mcnichol, J, Kujawinski, EB and **Sievert, SM.** 2018. Targeted metabolomics reveals proline as a major osmolyte in the chemolithoautotroph *Sulfurimonas denitrificans*. *MicrobiologyOpen* **7**(4): e00586. DOI: https://doi.org/10.1002/mbo3.586

Greenway, H and **Setter, TL.** 1979. Accumulation of proline and sucrose during the first hours after transfer of *Chlorella emersonii* to high NaCl. *Funct Plant Biol* **6**(1): 69–79. DOI: https://doi.org/10.1071/PP9790069

Grossi, SM and **Sullivan, CW.** 1985. Sea ice microbial communities: The vertical zonation of diatoms in an Antarctic fast ice community. *J Phycol* **21**(3): 401–409. DOI: https://doi.org/10.1111/j.0022-3646.1985.00401.x

Guillard, RRL. 1975. Culture of phytoplankton for feeding marine invertebrates. In: Smith, WL and Chanley, MH (eds.), *Cult of Mar Invert Anim*, 26–60. New York, USA: Plenum Press. DOI: https://doi.org/10.1007/978-1-4615-8714-9_3

Günther, S and **Dieckmann, GS.** 2001. Vertical zonation and community transition of sea-ice diatoms in fast ice and platelet layer, Weddell Sea, Antarctica. *Ann Glaciol* **33**: 287–296. DOI: https://doi.org/10.3189/172756401781818590

Harrison, PJ, Waters, RE and **Taylor, FJR.** 1980. A broad spectrum artificial sea water medium for coastal and open ocean phytoplankton. *J Phycol* **16**(1): 28–35. DOI: https://doi.org/10.1111/j.0022-3646.1980.00028.x

Horner, RA. (ed.) 1985. *Sea ice biota*. Boca Raton, FL: CRC Press.

Horner, RA and **Schrader, GC.** 1982. Relative contributions of ice algae, phytoplankton, and benthic microalgae to primary production in nearshore regions of the Beaufort Sea. *Arctic* **35**(4): 485–503. DOI: https://doi.org/10.14430/arctic2356

Hsiao, SIC. 1980. Quantitative composition, distribution, community structure and standing stock of sea ice microalgae in the Canadian Arctic. *Arctic* **33**(4): 768–793. DOI: https://doi.org/10.14430/arctic2595

Junge, K, Eicken, H and **Deming, JW.** 2004. Bacterial Activity at −2 to −20°C in Arctic wintertime sea ice. *Appl Environ Microbiol* **70**(1): 550–557. DOI: https://doi.org/10.1128/AEM.70.1.550-557.2004

Karsten, U, Kück, K, Vogt, C and **Kirst, GO.** 1996. Dimethylsulfoniopropionate production in phototrophic organisms and its physiological functions as a cryoprotectant. In: Kiene, RP, Vissher, PT, Keller, MD and Kirst, GO (eds.), *Biological and environmental chemistry of DMSP and related sulfonium compounds*, 143–153. Boston, MA: Springer US. DOI: https://doi.org/10.1007/978-1-4613-0377-0_13

Kattner, G, Thomas, DN, Haas C, Kennedy, H and **Dieckmann, GS.** 2004. Surface ice and gap layers in Antarctic sea ice: highly productive habitats. *Mar Ecol Prog Ser* **277**: 1–12. DOI: https://doi.org/10.3354/meps277001

Keller, MD, Matrai, PA, Kiene, RP and **Bellows, WK.** 2004. Responses of coastal phytoplankton populations to nitrogen additions: dynamics of cell-associated dimethylsulfoniopropionate (DMSP), glycine betaine (GBT), and homarine. *Can J Fish Aquat Sci* **61**(5): 685–699. DOI: https://doi.org/10.1139/f04-058

Kiene, RP and **Hoffmann Williams, LP.** 1998. Glycine betaine uptake, retention, and degradation by microorganisms in seawater. *Limnol Oceanogr* **43**(7): 1592–1603. DOI: https://doi.org/10.4319/lo.1998.43.7.1592

Kirst, GO, Thiel, C, Wolff, H, Nothnagel, J, Wanzek, M and **Ulmke, R.** 1991. Dimethylsulfoniopropionate (DMSP) in ice algae and its possible biological role. *Mar Chem* **35**(1–4): 381–388. DOI: https://doi.org/10.1016/S0304-4203(09)90030-5

Kohlbach, D, Lange, BA, Schaafsma, FL, David, C, Vortkamp, M, Graeve, M, van Franeker, JA, Krumpen, T and **Flores, H.** 2017. Ice algae-produced carbon is critical for overwintering of Antarctic krill *Euphausia superba*. *Front Mar Sci* **4**: 310. DOI: https://doi.org/10.3389/fmars.2017.00310

Kottmeier, ST and **Sullivan, CW.** 1987. Late winter primary production and bacterial production in sea ice and seawater west of the Antarctic Peninsula. *Mar Ecol Prog Ser* **36**(3): 287–298. DOI: https://doi.org/10.3354/meps036287

Krell, A, Funck, D, Plettner, I, John, U and **Dieckmann, G.** 2007. Regulation of proline metabolism under salt stress in the psychrophilic diatom *Fragilariopsis cylindrus* (Bacillariophyceae). *J Phycol* **43**(4): 753–762. DOI: https://doi.org/10.1111/j.1529-8817.2007.00366.x

Krembs, C, Eicken, H and **Deming, JW.** 2011. Exopolymer alteration of physical properties of sea ice and implications for ice habitability and biogeochemistry in a warmer Arctic. *PNAS* **108**(9): 3653–3658. DOI: https://doi.org/10.1073/pnas.1100701108

Krembs, C, Eicken, H, Junge, K and **Deming, JW.** 2002. High concentrations of exopolymeric substances in Arctic winter sea ice: Implications for the polar ocean carbon cycle and cryoprotection

of diatoms. *Deep Res Part I Oceanogr Res Pap* **49**(12): 2163–2181. DOI: https://doi.org/10.1016/S0967-0637(02)00122-X

Landa, M, Burns, AS, Durham, BP, Esson, K, Nowinski, B, Sharma, S, Vorobev, A, Nielsen, T, Kiene, RP and **Moran, MA.** 2019. Sulfur metabolites that facilitate oceanic phytoplankton–bacteria carbon flux. *ISME J* **13**(10): 2536–2550. DOI: https://doi.org/10.1038/s41396-019-0455-3

Landa, M, Burns, AS, Roth, SJ and **Moran, MA.** 2017. Bacterial transcriptome remodeling during sequential co-culture with a marine dinoflagellate and diatom. *ISME J* **11**(12): 2677–2690. DOI: https://doi.org/10.1038/ismej.2017.117

Lizotte, MP. 2001. The contributions of sea ice algae to Antarctic marine primary production. *Am Zool* **41**(1): 57–73. DOI: https://doi.org/10.1093/icb/41.1.57

Lu, X, Heal, KR, Ingalls, AE, Doxey, AC and **Neufeld, JD.** 2019. Metagenomic and chemical characterization of soil cobalamin production. *ISME J* **14**(1): 53–66. DOI: https://doi.org/10.1038/s41396-019-0502-0

Lyon, BR, Bennett-Mintz, JM, Lee, PA, Janech, MG and **Ditullio, GR.** 2016. Role of dimethylsulfoniopropionate as an osmoprotectant following gradual salinity shifts in the sea-ice diatom *Fragilariopsis cylindrus*. *Environ Chem* **13**(2): 181–194. DOI: https://doi.org/10.1071/EN14269

Lyon, BR, Lee, PA, Bennett, JM, DiTullio, GR and **Janech, MG.** 2011. Proteomic analysis of a sea-ice diatom: Salinity acclimation provides new insight into the dimethylsulfoniopropionate production pathway. *Plant Physiol* **157**(4): 1926–1941. DOI: https://doi.org/10.1104/pp.111.185025

Lyon, BR and **Mock, T.** 2014. Polar microalgae: New approaches towards understanding adaptations to an extreme and changing environment. *Biology* **3**(1): 56–80. DOI: https://doi.org/10.3390/biology3010056

MacLean, B, Tomazela, DM, Shulman, N, Chambers, M, Finney, GL, Frewen, B, Kern, R, Tabb, DL, Liebler, DC and **MacCoss, MJ.** 2010. Skyline: An open source document editor for creating and analyzing targeted proteomics experiments. *Bioinformatics* **26**(7): 966–968. DOI: https://doi.org/10.1093/bioinformatics/btq054

Michel, C, Nielsen, TG, Nozais, C and **Gosselin, M.** 2002. Significance of sedimentation and grazing by ice micro- and meiofauna for carbon cycling in annual sea ice (northern Baffin Bay). *Aquat Microb Ecol* **30**(1): 57–68. DOI: https://doi.org/10.3354/ame030057

Nothnagel, J. 1995. The effects of salinity and light intensity on the osmolyte concentrations, cell volumes and growth rates of the Antarctic sea-ice diatoms *Chaetoceros* sp. and *Navicula* sp. with emphasis on the amino acid proline [dissertation]. Bremen, DE: University of Bremen, Dept. of Biology/Chemistry and Marine Botany. *Rep Polar Res* **161**.

O'Brien, DP. 1987. Direct observations of the behavior of *Euphausia superba* and *Euphausia crystallorophias* (Crustacea: Euphausiacea) under pack ice during the Antarctic spring of 1985. *J Crustacean Biol* **7**(3): 437–448. DOI: https://doi.org/10.2307/1548293

Olenina, I, Hajdu, S, Edler, L, Andersson, A, Wasmund, N, Göbel, J, Huttunen, M, Jaanus, A, Legaine, I, Huseby, S and **Niemkiewicz, E.** 2006. Biovolumes and size-classes of phytoplankton in the Baltic Sea. *HELCOM Balt Sea Environ Proc* **106**: 1–144.

Reed, RH, Richardson, DL, Warr, SRC and **Stewart, WDP.** 1984. Carbohydrate accumulation and osmotic stress in cyanobacteria. *J Gen Microbiol* **130**(1): 1–4. DOI: https://doi.org/10.1099/00221287-130-1-1

Retelletti Brogi, S, Ha, SY, Kim, K, Derrien, M, Lee, YK and **Hur, J.** 2018. Optical and molecular characterization of dissolved organic matter (DOM) in the Arctic ice core and the underlying seawater (Cambridge Bay, Canada): Implication for increased autochthonous DOM during ice melting. *Sci Total Environ* **627**: 802–811. DOI: https://doi.org/10.1016/j.scitotenv.2018.01.251

Riaux-Gobin, C, Poulin, M, Dieckmann, G, Labrune, C and **Vétion, G.** 2011. Spring phytoplankton onset after the ice break-up and sea-ice signature (Adélie Land, East Antarctica). *Polar Res* **30**(1): 5910. DOI: https://doi.org/10.3402/polar.v30i0.5910

Scholz, B and **Liebezeit, G.** 2012. Compatible solutes in three marine intertidal microphytobenthic Wadden Sea diatoms exposed to different salinities. *Eur J Phycol* **47**(4): 393–407. DOI: https://doi.org/10.1080/09670262.2012.720714

Slama, I, Abdelly, C, Bouchereau, A, Flowers, T and **Savouré, A.** 2015. Diversity, distribution and roles of osmoprotective compounds accumulated in halophytes under abiotic stress. *Ann Bot* **115**(3): 433–447. DOI: https://doi.org/10.1093/aob/mcu239

Spielmeyer, A, Gebser, B and **Pohnert, G.** 2011. Investigations of the uptake of dimethylsulfoniopropionate by phytoplankton. *ChemBioChem* **12**(15): 2276–2279. DOI: https://doi.org/10.1002/cbic.201100416

Spielmeyer, A and **Pohnert, G.** 2012. Influence of temperature and elevated carbon dioxide on the production of dimethylsulfoniopropionate and glycine betaine by marine phytoplankton. *Mar Environ Res* **73**: 62–69. DOI: https://doi.org/10.1016/j.marenvres.2011.11.002

Spietz, RL, Lundeen, RA, Zhao, X, Nicastro, D, Ingalls, AE and **Morris, RM.** 2019. Heterotrophic carbon metabolism and energy acquisition in *Candidatus* Thioglobus singularis strain PS1, a member of the SUP05 clade of marine *Gammaproteobacteria*. *Environ Microbiol* **21**(7): 2391–2401. DOI: https://doi.org/10.1111/1462-2920.14623

Tedesco, L, Vichi, M and **Thomas, DN.** 2012. Process studies on the ecological coupling between sea ice algae and phytoplankton. *Ecol Modell*

226: 120–138. DOI: https://doi.org/10.1016/j.ecolmodel.2011.11.011

Torstensson, A, Hedblom, M, Andersson, J, Andersson, MX and **Wulff, A.** 2013. Synergism between elevated pCO_2 and temperature on the Antarctic sea ice diatom *Nitzschia lecointei*. *Biogeosciences* **10**(10): 6391–6401. DOI: https://doi.org/10.5194/bg-10-6391-2013

Torstensson, A, Young, JN, Carlson, LT, Ingalls, AE and **Deming, JW.** 2019. Use of exogenous glycine betaine and its precursor choline as osmoprotectants in Antarctic sea-ice diatoms. *J Phycol* **70**: 1–13. DOI: https://doi.org/10.1111/jpy.12839

UNESCO. 1994. Protocols for the joint global ocean flux study (JGOFS) core measurements. *IOC Manuals and Guides* **29**.

van Leeuwe, MA, Tedesco, L, Arrigo, KR, Assmy, P, Campbell, K, Meiners, KM, Rintala, J-M, Selz, V, Thomas, DN and **Stefels, J.** 2018. Microalgal community structure and primary production in Arctic and Antarctic sea ice: A synthesis. *Elem Sci Anth* **6**. DOI: https://doi.org/10.1525/elementa.267

Vancoppenolle, M, Meiners, KM, Michel, C, Bopp, L, Brabant, F, Carnat, G, Delille, B, Lannuzel, D, Madec, G, Moreau, S, Tison, JL and **van der Merwe, P.** 2013. Role of sea ice in global biogeochemical cycles: Emerging views and challenges. *Quat Sci Rev* **79**: 207–230. DOI: https://doi.org/10.1016/j.quascirev.2013.04.011

Warr, SRC, Reed, RH and **Stewart, WDP.** 1984. Osmotic adjustment of cyanobacteria: The effects of NaCl, KCl, sucrose and glycine betaine on glutamine synthetase activity in a marine and a halotolerant strain. *J Gen Microbiol* **130**(9): 2169–2175. DOI: https://doi.org/10.1099/00221287-130-9-2169

Welschmeyer, NA. 1994. Fluorometric analysis of chlorophyll a in the presence of chlorophyll b and pheopigments. *Limnol Oceanogr* **39**(8): 1985–1992. DOI: https://doi.org/10.4319/lo.1994.39.8.1985

Welsh, DT. 2000. Ecological significance of compatible solute accumulation by micro-organisms: from single cells to global climate. *FEMS Microbiol Rev* **24**(3): 263–290. DOI: https://doi.org/10.1111/j.1574-6976.2000.tb00542.x

Yancey, PH. 2005. Organic osmolytes as compatible, metabolic and counteracting cytoprotectants in high osmolarity and other stresses. *J Exp Biol* **208**(15): 2819–2830. DOI: https://doi.org/10.1242/jeb.01730

Yancey, PH, Clark, ME, Hand, SC, Bowlus, RD and **Somero, GN.** 1982. Living with water stress: Evolution of osmolyte systems. *Science*. **217**(4566): 1214–1222. DOI: https://doi.org/10.1126/science.7112124

How to cite this article: Dawson, HM, Heal, KR, Boysen, AK, Carlson, LT, Ingalls, AE and Young, JN. 2020. Potential of temperature- and salinity-driven shifts in diatom compatible solute concentrations to impact biogeochemical cycling within sea ice. *Elem Sci Anth,* 8: 25. DOI: https://doi.org/10.1525/elementa.421

Domain Editor-in-Chief: Detlev Helmig, Institute of Alpine and Arctic Research, University of Colorado Boulder, US

Associate Editor: Kevin Arrigo, Environmental Earth System Science, Stanford University, US

Knowledge Domain: Ocean Science

Submitted: 01 November 2019 **Accepted:** 05 May 2020 **Published:** 19 June 2020

ELEMENTA Science of the Anthropocene

Elem Sci Anth is a peer-reviewed open access journal published by University of California Press.

OPEN ACCESS